Received: 25 September 2018 | Accepted: 28 January 2019
DOI: 10.1002/hyp.13405

RESEARCH ARTICLE

WILEY

Assessing urban flood and drought risks under climate change, China

Chen Liang | Dingqiang Li | Zaijian Yuan | Yishan Liao | Xiaodong Nie | Bin Huang | Xinliang Wu | Zhenyue Xie

Guangdong Key Laboratory of Integrated Agro-environmental Pollution Control and Management, Guangdong Institute of Eco-environmental Science and Technology, Guangzhou, China

Correspondence
Zaijian Yuan, Guangdong Key Laboratory of Integrated Agro-environmental Pollution Control and Management, Guangdong Institute of Eco-environmental Science and Technology, Guangzhou 510650, China.
Email: zjyuan@soil.gd.cn

Funding information
Science and Technology Planning Project of Guangdong Province, Grant/Award Numbers: 2017A070702015 and 2017B030314092; Guangzhou Science and Technology Plan Project, Grant/Award Number: 201707010408; High-level Leading Talent Introduction Program of GDAS, Grant/Award Number: 2016GDASRC-0103; GDAS' Project of Science and Technology Development, Grant/Award Numbers: 2018GDASCX-0106, 2019GDASYL-0401003, 2019GDASYL-0502004 and 2019GDASYL-0503003

Abstract

Risk analysis of urban flood and drought can provide useful guidance for urban rainwater management. Based on an analysis of urban climate characteristics in 2,264 Chinese cities from 1958 to 2017, this study evaluated urban flood and drought risks. The results demonstrated that the annual average values of precipitation, aridity index, frequency and intensity of extreme precipitation and extreme drought events differed significantly in these cities. The values of the above six climatic indicators in the cities ranged from 9.29–2639.30 mm, 0.47–54.73, 1.08–8.79 time, 7.82–107.25 mm, 0.76–2.99 time, and 10.30–131.19 days, respectively. The geographical patterns of urban precipitation, aridity index, intensity and frequency of extreme precipitation and drought events in China fit well to the Hu-Huanyong Line that was created in 1940s to identify the pattern of population distribution. Extreme precipitation in most cities has upward trends, except for those around the Hu-Huanyong Line. The extreme drought events had upward trends in the cities east of the Hu-Huanyong Line, but there were downward trends in the cities west of the line. The risk assessment indicated that 3.80% cities were facing serious flood and 6.01% cities were facing serious drought risks, which are located in the coast of southern China and northwestern China, respectively, and other 90.19% cities were facing different types of drought and flood risks in terms of their intensity and frequency.

KEYWORDS

drought, flood, rainwater management, risk, urban climate change

1 | INTRODUCTION

Climate change is one of the most imminent threats to human society and has great impacts on normal living and security of urban systems. Due to the effects of climate change, extreme meteorological events, such as droughts, floods, rainstorms, and tropical typhoons, have occurred more frequently in recent years, which has seriously affected human daily life and economic production (Dao & Hoang, 2016; Pachauri et al., 2014). In recent years, some studies have discussed the interference of climate change on urban economy and people's lives (Hallegatte, Hourcade, & Ambrosi, 2007; Mishra, Ganguly, Nijssen, & Lettenmaier, 2015; Rosenzweig, Solecki, Hammer, & Mehrotra, 2010). With the expansion of urbanization, many problems such as drought, flood, and water pollution have become serious, and climate change aggravates these matters.

Presently, many researches established models by using remote sensing and geographic information system technology to dynamically simulate the urban flooding process (Bernardini et al., 2017; Guidolin et al., 2016; Meesuk, Vojinovic, Mynett, & Abdullah, 2015; Smith, Liang, & Quinn, 2015), to analyse the mechanism of urban waterlogging (S. Du, Shi, Van Rompaey, & Wen, 2015; L. Yao, Wei, & Chen, 2016), to evaluate the characteristics of the risk of

waterlogging (Chang & Huang, 2015; H. Huang et al., 2017), and to design the urban drainage system (Duan, Li, & Yan, 2016; Smith et al., 2015). These models included hydrologic models and digital surface and terrain models. On the other hand, many indicators were adopted to analyse the temporal and spatial characteristics of urban drought and flood (J. Du, Fang, Xu, & Shi, 2013; Gober, Sampson, Quay, White, & Chow, 2016; Ortega-Gómez, Pérez-Martín, & Estrela, 2018) and to discuss the impacts of drought and flood on natural environment and human life (Miller & Hutchins, 2017; Tortajada, Kastner, Buurman, & Biswas, 2017).

In China, many cities, such as Beijing, Guangzhou, Wuhan, Shijiazhuang, and Shenzhen (Figure 1), have frequently experienced urban floods and droughts (Shao et al., 2016). For example, in August 2007, Changsha suffered a severe once-in-50-years drought because of continuous high temperatures and little precipitation. Many rivers, such as the Xiangjiang River, dried up, which threatened the supply of drinking water for a million residents (http://news.sina.com.cn/c/2007-08-07/115512342131s.shtml). On July 6, 2016, heavy rain came to Wuhan with 184 mm of rainfall in a single day; the rainstorm caused traffic paralysis, and the waiting room of Wuhan Railway Station was flooded (http://www.88148.com/News/2016070647902.html). In the morning of May 10, 2016, Guangzhou encountered a heavy rain with 81.4 mm rainfall in 2 hr; the city was flooded, and the rainwater ran into the subway (http://news.ifeng.com/a/20160511/48752010_0.shtml). Because of days of rain during June 2017 in Changsha and its surrounding areas, Orange Island was flooded on July 2, 2017 (http://photos.caixin.com/2017-07-03/101109607.html). These disasters have caused serious economic losses plus human death or injury, and the situation is escalating steeply (Zou, Xu, & Qiu, 2015). More frequent and severe floods and droughts will raise higher demand for basic clean water supplies in cities (Rosenzweig et al., 2010). With the rapid expansion of urbanization, the total building floor area constructed in China over the last decade has been more than three times that over the past 46 years (Qian, 2016). Overall, urban flood and drought hazards will increase in the future even without considering the potential impacts of climate change (Güneralp, Güneralp, & Liu, 2015).

To strengthen the management and utilization of urban rainwater resources, China began to implement a "sponge city" construction programme in 2014 (Shao et al., 2016). "Sponge city" means that cities can absorb, store, purify, seep, and release rainwater such as sponges, which emphasizes the concept of "natural accumulation, natural infiltration and natural purification." Now, there are 30 cities (e.g., Ji'nan, Wuhan, Xiamen, Beijing, Tianjin, and Shanghai; Figure 1) that have carried out the construction of sponge city, but the research on sponge city in China has emphasized engineering measures while ignoring nonengineering measures (Yang, Scheffran, Qin, & You, 2015). The construction of sponge city should consider climate

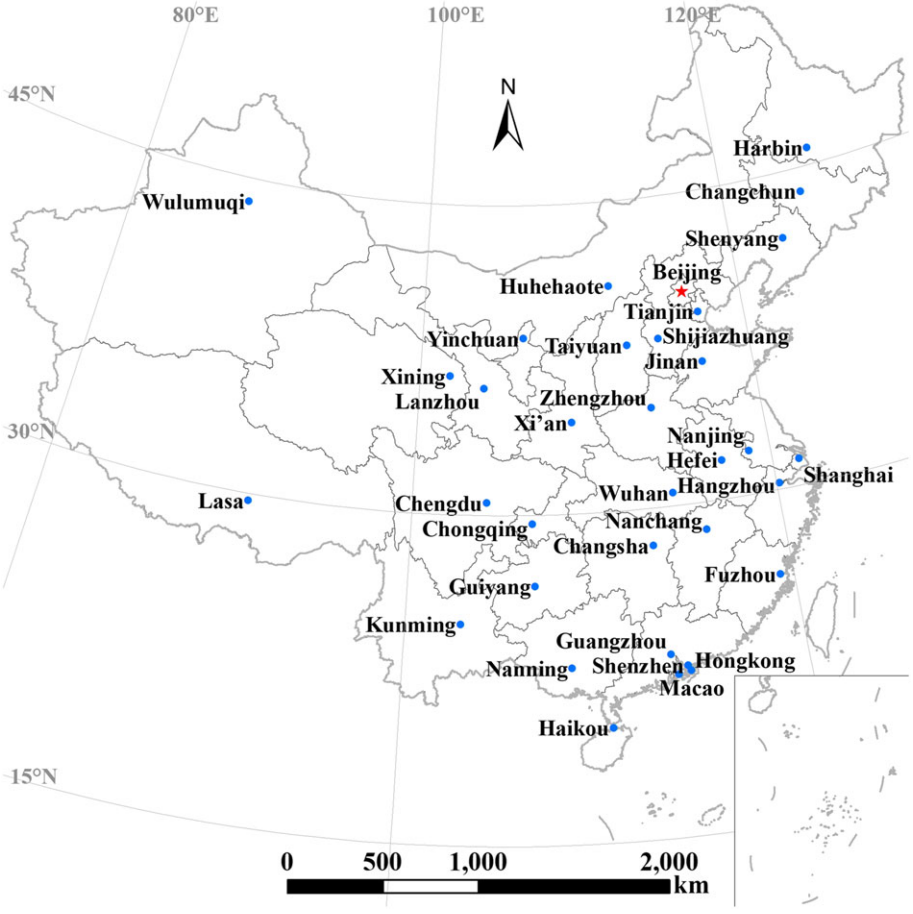

FIGURE 1 Distribution of main cities in China

change, and the corresponding measures should be proposed to deal with climate change. Therefore, the main objectives of this study were to (a) discuss the characteristics of the urban climate change over the past 60 years (1958–2017) in China and (b) estimate the risk of flood (especially caused by local heavy precipitation) and drought in the near future (2018–2027) in these cities.

2 | MATERIALS AND METHODS

2.1 | Data

To perform this research, meteorological data were provided by China Meteorological Administration from 566 stations across China (Figure 2) for the period 1958–2017, including daily average temperature, relative humidity, precipitation, sunshine duration, atmospheric pressure, vapour pressure, and wind speed (China Meteorological Administration, 1958–2017). The information of cities at county level (including number, name, and location of the cities) came from the statistical yearbooks of China (2016). In addition, this paper used four extreme event indicators and many abbreviations, which were showed in Table 1.

2.2 | Introduction of the Hu-Huanyong Line

The Hu-Huanyong Line was put forward by Hu Huanyong in 1935, which was connected from Heihe (Aihui) city of Heilongjiang province to Tengchong county of Yunnan province. This line can divide the population distribution in China, and it basically coincided with the 400-mm precipitation isoline. According to the statistical data in 2010, the southeast side of the Hu-Huanyong Line (except for Hong Kong, Macao, and Taiwan province) covered 36% of the total area of mainland and has gathered 94% of the population and contributed to 95.70% of the national gross domestic product in China. Therefore, this line can be regarded as an important geographical, economic, and social division line in China (S. Liu et al., 2017; Qi, Liu, & Zhao, 2015).

2.3 | Relevant methods

In this study, the values of urban climate indicators can be obtained by Kriging interpolation using meteorological data. The MK test (Kendall, 1975; Mann, 1945) with the trend-free pre-whitening (TFPW; S. Yue, Pilon, Phinney, & Cavadias, 2002) procedure was used to detect climatic indicators trends, and the K-means clustering (Macqueen,

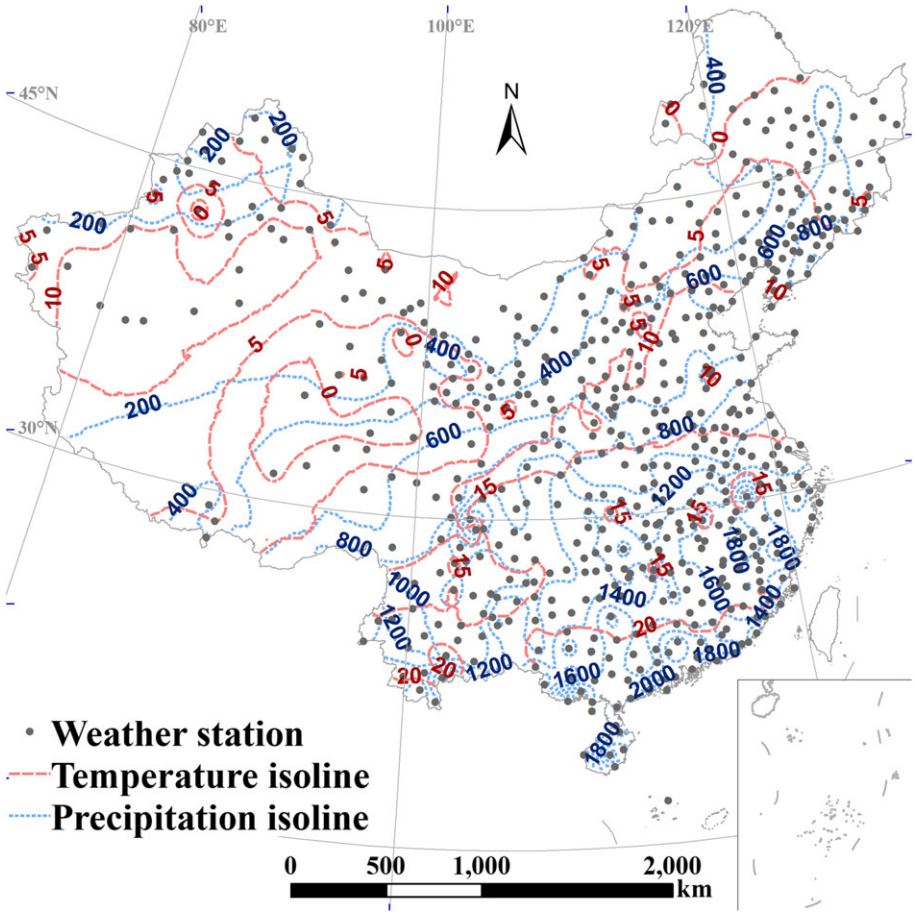

FIGURE 2 Contour lines indicate average precipitation and average temperature (1958–2017), respectively, and the points indicate the locations of weather stations

TABLE 1 Abbreviation and meaning of indices applied in this study

Indices (unit)	Meaning
Pre (mm)	Annual total precipitation
AI (dimensionless)	Aridity index
EPF (time)	Extreme precipitation frequency, that is, the number of extreme precipitation events occurring in the year
EPI (mm)	Extreme precipitation intensity, that is, the ratio of total intensity to the occurrence frequency of extreme precipitation events during the year
EDF (time)	Extreme drought frequency, that is, the number of extreme drought events occurring in the year
EDI (d)	Extreme drought intensity, that is, the ratio of total intensity to the occurrence frequency of extreme drought events during the year
APVAI (dimensionless)	The average of predicted value of AI in the next 10 years (i.e., the mean value of AI from 2017 to 2026, calculated by linear regression)
APVEPF (time)	Same as above, but for EPF
APVEPI (mm)	Same as above, but for EPI
APVEDF (time)	Same as above, but for EDF
APVEDI (days)	Same as above, but for EDI

1967) was used to classify cities according to their risk characteristics. In order to identify the risk characteristics of urban drought and flood, AI, EPF, EPI, EDF, and EDI were chosen to reflect the general and extreme climate characteristics, and linear regression was used to calculate the predicted mean value of each index in the next 10 years (2018–2027) for each city, which are defined as APVAI, APVEPF, APVEPI, APVEDF, and APVEDI, respectively. Based on the above indicators, the risk classification of urban drought and flood was analysed by K-means clustering method, and in order to balance the accuracy and difference of classification results, the cities were divided into six categories. In addition, the six cluster centres of each index were divided into three categories by the K-means method, that is, high, medium, and low, to reflect the types of risk.

2.4 | Aridity index

Aridity index reflects climatic dry or wet conditions in specific region. A common form of meteorological aridity can be expressed as the ratio of annual total potential evaporation to annual total precipitation (Budyko, 1974; Meng, Ni, & Zhang, 2004), which can accurately show the difference in water balance between each city in our study:

$$AI = \frac{ET_p}{Pre}, \tag{1}$$

where ET_p is the annual total potential evapotranspiration (mm). In a broad sense, the value of *AI* can define climate regimes, such as superarid (AI $\geq$ 30), hyper-arid (30 > AI $\geq$ 12), arid (12 > AI $\geq$ 5), semi-arid (5 > AI $\geq$ 2), subhumid (2 > AI $\geq$ 0.75), humid (0.75 > AI $\geq$ 0.375), and hyper-humid (AI < 0.375; Ponce, Pandey, & Ercan, 2000).

ET_p represents the maximum possible water evaporation in a period (in this paper, for 1 year), which can be calculated by Penman formula (Brutsaert, 2005; Penman, 1948):

$$ET_p = \frac{\Delta \quad R_n}{\Delta + \gamma\,\lambda} + \frac{\gamma}{\Delta} + \gamma E_A, \tag{2}$$

$$E_A = f(u_2)(e_s - e_a), \tag{3}$$

$$f(u_2) = 0.26(1 + 0.54u_2), \tag{4}$$

where Δ is the slope of the curve of vapour pressure versus temperature, R_n represents the net radiation at the reference surface, γ represents the psychrometric constant, λ is the latent heat of vaporization, E_A is the drying power of the air, u_2 represents the wind speed at 2-m height, e_s is the saturated vapour pressure, and e_a represents the actual vapour pressure. More detail calculation method of these parameters can be found in previous papers (Allen, Pereira, Raes, & Smith, 1998; Yuan, Liang, & Li, 2018). The data required for this calculation, including daily temperature, relative humidity, precipitation, sunshine duration, atmospheric pressure, vapour pressure, and wind speed, were derived from meteorological station, and all constants used the values recommended by the references (Allen et al., 1998; Brutsaert, 2005).

2.5 | Extreme precipitation and extreme drought

Extreme precipitation (EP) events were usually defined as a daily precipitation exceed a certain threshold, and this threshold was generally calculated by the method of specific quantiles of daily precipitation series (Groisman et al., 1999). In this study, according to the cumulative probability distribution of daily precipitation during the standard time (1971–2000, recommended by the World Meteorological Organization), the threshold of extreme precipitation events is defined as the daily precipitation value with a cumulative probability of 95%. Therefore, the probability of extreme precipitation events was 5% in standard time period, and from 1958 to 2016, the daily precipitation events that exceeding the threshold are defined as extreme precipitation event.

Referencing the definition of consecutive dry days (CDD, the number of consecutive days when the precipitation is less than 0.1 mm/day) proposed by Frich et al. (2002), the extreme drought (ED) event was defined by the use of the inverse cumulative probability distribution function of CDD (regard adjacent years as continuous data, and the time of the occurrence of a drought event is defined as the start date of CDD); during the standard time period, the threshold of extreme drought events is defined as the CDD with an inverse cumulative

probability distribution function value of 5%. So the probability of extreme drought events in the standard time period is also 5%. According to our calculation, the threshold of EP in 2,264 cities ranges from 5.79 to 76.02 mm, with an average value of 31.88 mm; the threshold of ED ranges from 6.14 to 182.32 days, with an average of 20.97 days.

3 | RESULTS

3.1 | Spatial characteristics of the main urban climatic indicators

The average of Pre, AI, EPF, EPI, EDF, and EDI in each city from 1958 to 2017 was calculated, and the results indicated that the spatial distribution of urban climate characteristics has specific pattern in China. (a) The average annual Pre of the 2,264 cities ranged from 9.29 mm (in Tulufan city of Xinjiang Uygur Autonomous Region) to 2,639.30 mm (in Dongxing city of Guangxi province), and the corresponding value of 1,836 cities (approximately 81% of cities) was above 500 mm, most of which were located in the southeast of the Hu-Huanyong Line (Figure 3a). (b) The average annual AI ranged from 0.47 (in Dongxing city of the Guangxi Zhuang Autonomous Region) to 54.73 (in Tulufan city) with approximately 85% of cities lower than 2, and most humid and subhumid cities were located in the southeast of the Hu-Huanyong Line (Figure 3b). (c) The average annual EPF ranged from 1.08 time (in Ruoqiang county of Xinjiang) to 8.79 time (in Junlian county of Sichuan province) with approximately 73% cities above 4 time (Figure 3c). The average annual EPI ranged from 7.82 mm (in Ruoqiang county) to 107.25 mm (in Sansha city of Hainan province) with approximately 74% cities above 40 mm, and most of which were

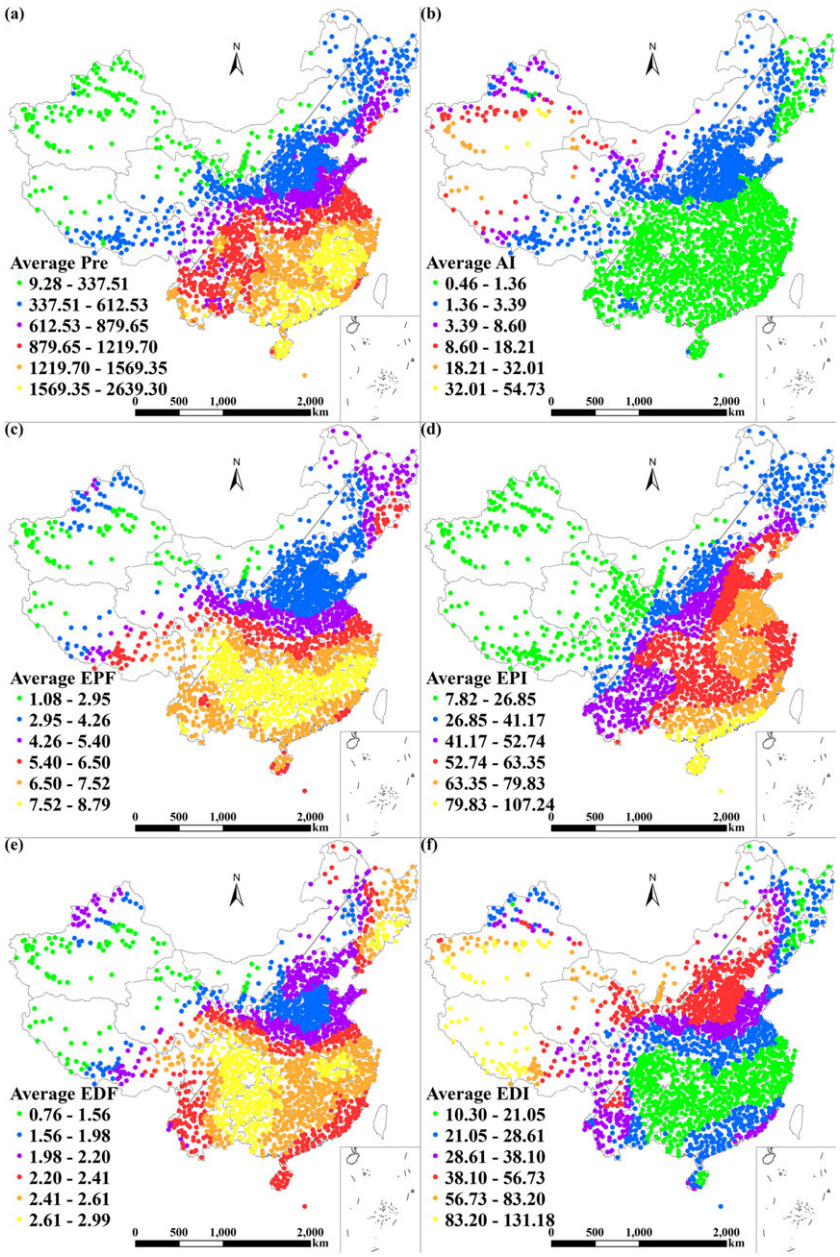

FIGURE 3 The spatial distribution of the average climatic indicator values in the cities of China: average of (a) Pre, (b) AI, (c) EPF, (d) EPI, (e) EDF, and (f) EDI from 1958 to 2016. The segment line is the Hu-Huanyong Line

located in the southeast of the Hu-Huanyong Line (Figure 3d). (d) The average annual EDF ranged from 0.76 time (in Ruoqiang county) to 2.99 time (in Changbai county of Jilin province) with approximately 78% cities above 2 time (Figure 3e). The average annual EDI ranged from 10.30 days (in Xuyong county of Sichuan province) to 131.19 days (in Shigatse city of Tibet Autonomous Region), with approximately 93% cities lower than 50 days, and most of which were located in the southeast of the Hu-Huanyong Line, too (Figure 3f).

3.2 | Trends of urban climate change in China

Climate change characteristics are checked by index TFPW-MK trend test from 1958 to 2017 (with α = 0.05) in each city. The results indicated that (a) Pre showed a nonsignificant trend in 88.47% cities throughout the country, and approximately half of the cities showed an upward trend (Table 2). The cities with significant Pre upward trends were mainly distributed in the northwest of the Yangtze River Delta, whereas the cities with significant downward trends were mainly located in Yunnan, Sichuan, and Shandong provinces (Figure 4a). (b) AI of more than half cities showed a nonsignificant downward trend, and about one third cities had nonsignificant upward trends (Table 2), which are mainly located around the Hu-Huanyong Line (Figure 4b). Generally, the AI trend was mainly opposite to Pre trend, especially in the cities west of the Hu-Huanyong Line showed a downward AI trend, and the cities in Sichuan, Yunnan, and Ningxia had an upward AI trend (Figure 4b), whereas the Pre in these cities showed an opposite trend (Figure 4a). This phenomenon meant that the change of precipitation can primarily affect the trend of AI. However, there are a few exceptions, such as some cities in Hebei, Shandong, and Shanxi Henan provinces showed nonsignificant downward trends in Pre and AI. Although the precipitation was decreasing in these cities, the reduction of evapotranspiration may be more obvious, so that they were still in a more humid trend on the whole (Figure 4b). (c) For extreme precipitation, there were 64.53% and 71.16% of the cities in China that had an upward trend of EPF and EPI, respectively. Among them, cities in west of the Hu-Huanyong Line mainly had an upward trend of EPF and EPI at the same time, especially in Xinjiang, Gansu, and Qinghai provinces. EPF and EPI in most cities of North China Plain and Northeast Plain showed downward trend. Except for some cities in Sichuan and Yunnan Province, most of the cities in Southern China had upward trends of EPF, particularly in the middle and lower reaches of the Yangtze River, whereas except for a few cities in Guangdong and Yunnan provinces, the EPI of most cities in south China showed an upward trend or even significant upward trends (Figure 4c,d). (d) In terms of extreme drought, about 75.18% and 63.52% of the cities in China have upward trends in EDF and EDI, respectively. Interestingly, the frequency and intensity of extreme drought had declined in most areas located in west of the Hu-Huanyong Line due to precipitation significant increase over the past 60 years. In east of the Hu-Huanyong Line, 71.11% cities had the same trend of EDF and EDI with upward trends. In the cities located in Sichuan, Yunnan, Guizhou, Guangxi, and Hainan provinces, the upward trends of EDF were significant, and the cities with significant upward EDI trends mainly distributed in this area too. The cities with downward trends of EDF are mainly distributed in northeast of China, Shanxi, Jiangxi, Anhui, and Shanghai, whereas the distribution of cities with significant EDI trends tends to be more fragmented (Figure 4e,f).

3.3 | Assessment of urban flood and drought risk

All cities were divided into six categories according to drought and flood risk types by cluster analysis (Table 3 and Figure 5); the characteristics of drought and flood risk in each type of city are shown in Table 4. The result indicated that the six types of cities (sorted by APVAI) reflected different patterns of drought and flood risk. Except APVEDF, the cluster centre values of the other four indexes are quite different. This indicates that APVAI, APVEPF, APVEPI, and APVEDI played key roles in the clustering process, and the frequency of extreme drought events was less important to classify the urban drought and flood risk. In addition, the number of the six types of cities was generally characterized by normal distribution; serious flood risk cities (the first category) and severe drought risk cities (sixth type) are relatively small; and the number of other mitigating situations is relatively large. Type 1 cities had humid climate with high APVEPF, APVEPI and low APVEDI. In the future, these cities will face serious flood risk. Such cities account for only 3.80% of the total, mainly located in the coastal areas of southern China. Type 2 and Type 3 cities have humid climate, which account for about 50% of the total. The risk types of drought are similar to those of the first category, and the intensity and frequency of flood are slightly reduced, but it is still the key point for prevention and control. These two types of cities are mainly distributed in the vast areas of south China, northeast China, and north China. Type 4 and Type 5 cities account for 39.00% of the total. Their dry and wet conditions of climate belong to the moderate level and have the same type of APVEPF, APVEDF, and APVEDI, whereas APVEPI value is slightly different. These two types of cities have mitigating risk of drought and flood, mainly located

TABLE 2 The number of cities with different climate trends

Trend type	Pre	AI	EPF	EPI	EDF	EDI
Significant downward	98	269	19	24	93	60
Non-significant downward	1044	1176	770	608	458	745
No trend	17	24	14	21	11	21
Non-significant upward	942	756	1044	1310	1134	1239
Significant upward	163	39	417	301	568	199

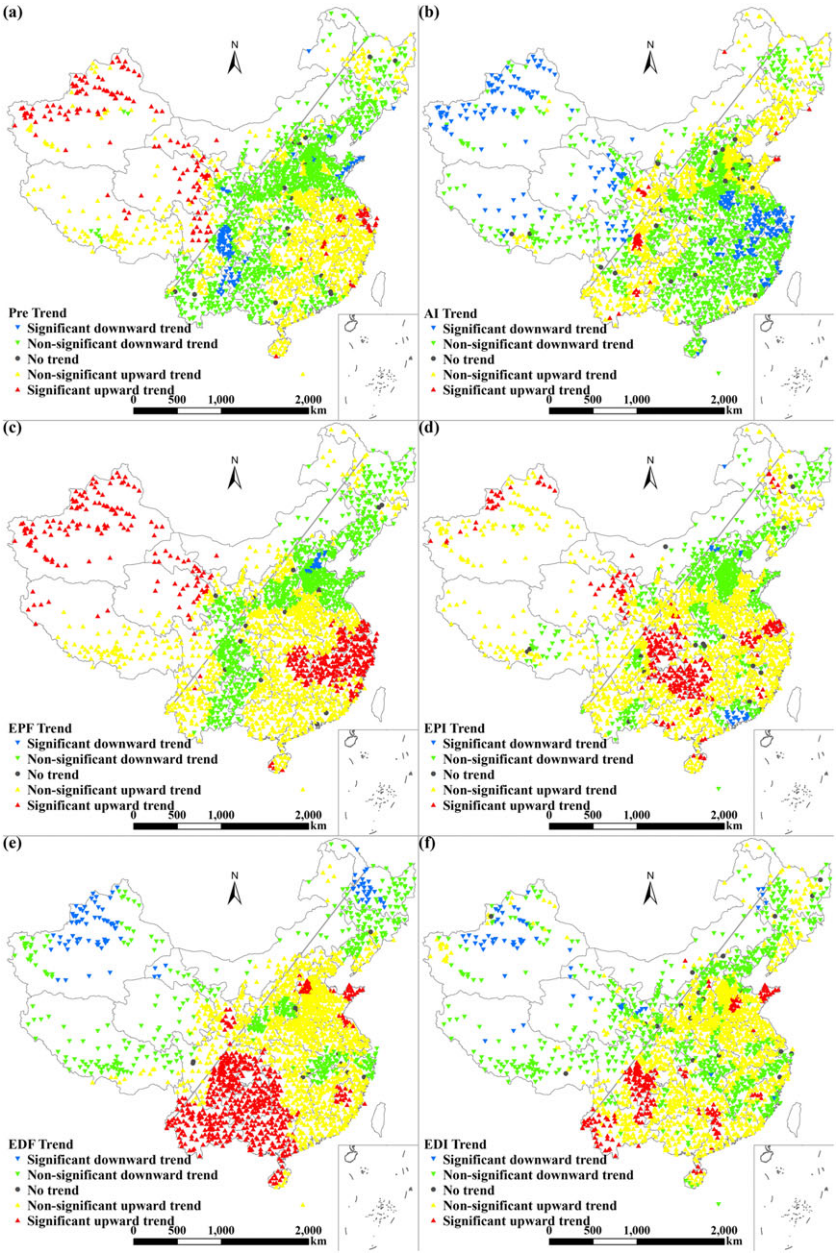

FIGURE 4 Trend of urban climatic indicators in China, (a) Pre, (b) AI, (c) EPF, (d) EPI, (e) EDF, and (f) EDI

around the Hu-Huanyong Line and northern Xinjiang. Type 6 cities account for 6.01% of the total, with the climate conditions are extremely dry. The risk types are characterized by low frequency and intensity of extreme precipitation event, low frequency but extremely high intensity of extreme drought event. These cities are mainly located in Xinjiang, Qinghai, Gansu, Inner Mongolia, and Shaanxi provinces of northwest China and Tibet Plateau.

4 | DISCUSSION

4.1 | Interaction of urbanization and climate change

Traditional grey drainage facilities (drainage system based on urban engineering pipeline; Vineyard et al., 2015) used in urban construction can effectively alleviate flood in some degree; however, with the continuous expansion of the urban area, they are often difficult to discharge the urban rainwater. On the other hand, the destruction of natural environment caused by the construction of impervious roads leads to the aggravation of nonpoint source pollution and increase of drought and flood events (S. Du et al., 2015; Q. Huang, Zhang, Singh, Shi, & Zheng, 2017). In addition, urbanization has a significant influence on climate (Kalnay & Cai, 2003; Golroudbary, Zeng, Mannaerts, & Su, 2017); by making urban temperature rise (Guo & Ya, 2014; Kalnay & Cai, 2003; Y. Z. Li, Luo, & Zhou, 2015; A. Y. Zhang et al., 2010), the urban heat-island effect is its most prominent characteristic (Manley, 1958; Jusuf, Wong, Hagen, Anggoro, & Hong, 2007). And the increase of extreme precipitation events is closely related with human activities and greenhouse gas emissions, because climate warming will lead to a more intense hydrological cycle in nature (Güneralp et al.,

TABLE 3 Clustering centres and risk types

Cluster center	APVAI	APVEPF	APVEPI	APVEDF	APVEDI	Number of cities
Type 1	0.77 (l)	7.39 (h)	92.46 (h)	2.84 (m)	26.55 (l)	86 (3.80%)
Type 2	0.87 (l)	7.10 (m)	66.08 (m)	2.70 (m)	23.30 (l)	733 (32.38%)
Type 3	0.99 (l)	7.18 (m)	51.60 (m)	3.05 (h)	19.90 (l)	426 (18.82%)
Type 4	1.69 (m)	4.11 (l)	48.80 (m)	2.24 (l)	42.17 (m)	512 (22.61%)
Type 5	2.17 (m)	4.99 (l)	26.77 (l)	2.14 (l)	32.38 (m)	371 (16.39%)
Type 6	9.30 (h)	3.75 (l)	17.56 (l)	1.34 (l)	69.24 (h)	136 (6.01%)

Note. "l," "m," and "h" means "low," "moderate," and "high," respectively. APVAI: average of predicted value of aridity index; APVEPF: average of predicted value of precipitation frequency; APVEPI: average of predicted value of precipitation intensity; APVEDF: average of predicted value of drought frequency; APVEDI: average of predicted value of drought intensity.

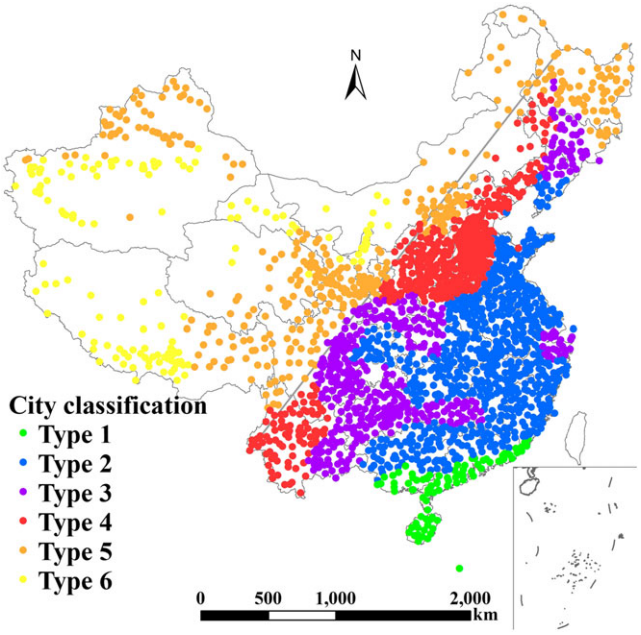

FIGURE 5 The distribution of the six types of cities

TABLE 4 Meaning of urban type

Types of city	Risk characteristics of drought and flood
Type 1	low APVAI, APVEDI + moderate APVEDF + high APVEPF, APVEPI
Type 2	low APVAI, APVEDI + moderate APVEPF, APVEPI, APVEDF
Type 3	low APVAI, APVEDI + moderate APVEPF, APVEPI + high APVEDF
Type 4	low APVEPF, APVEDF + moderate APVAI, APVEPI, APVEDI
Type 5	low APVEPF, APVEPI, APVEDF + moderate APVAI, APVEDI
Type 6	low APVEPF, APVEPI, APVEDF + high APVAI, APVEDI

Note. APVAI: average of predicted value of aridity index; APVEPF: average of predicted value of precipitation frequency; APVEPI: average of predicted value of precipitation intensity; APVEDF: average of predicted value of drought frequency; APVEDI: average of predicted value of drought intensity.

2015; Coumou & Rahmstorf, 2012). Therefore, climate change may cause extreme hydrologic events (including drought and flood) to happen more frequently (Zhou et al., 2011).

Urbanization affects the hydrological cycle significantly, and urban precipitation may increase with urbanization development (Bai et al., 2013; Liang, Ding, He, & Tang, 2011; Palumbo & Mozzarella, 1980; Shepherd, 2006). At the same time, abnormal changes of the hydrological cycle can seriously affect precipitation, evaporation, runoff, and river systems, which exacerbates the destruction of urban ecological environment. Urban climate change has a significant impact on the hydrologic cycle, too (Middelkoop et al., 2001; Yang, Chan, & Scheffran, 2018); urban flood and drought occur mainly because precipitation and drought extreme events exceed the capacity of urban infrastructure, and the current standard of urban infrastructure cannot cope with climate change and extreme climate events effectively.

The changes of urban extreme climate events are very complex and have received extensive research in recent years (T. Gao & Xie, 2016; S. Liu et al., 2017; Song et al., 2015; H. Wang et al., 2017; X. Wang, Hou, & Wang, 2017; Zhai, Zhang, Wan, & Pan, 2005; K. Zhang et al., 2014; Zhao, Zou, Cao, & Xu, 2014). In the future, without the infrastructure to deal with floods and droughts, the livelihoods and settlements of urban residents will be at medium- and high-risk level in Asia (Pachauri et al., 2014). Therefore, urban governments should consider the characteristics of the urban environment and climate change and try to adopt decentralized, source-based, green, low-impact development measures to reduce the impact of artificial facilities on the hydrological cycle processes during urban construction and management. Fortunately, many modern means of stormwater management, such as low impact development and green infrastructure, have been adopted, which can mitigate the risk of drought and flood comprehensively and improve the adaptability of cities to climate change (S. Du et al., 2015).

4.2 | Comparison with related researches

Compared with other researches, the mean and trend of precipitation, extreme precipitation events, and extreme drought events in this study are generally similar whereas the climate indicators are not absolutely identical. For example, using Standardized Precipitation Evapotranspiration Index based on Penman (SPEI-PM) representative evapotranspiration formula, Y. Chen, Zhou, Zhang, Du, and Zhou (2015) found that the climate in the vicinity of the Hu-Huanyong Line has a trend of drought, and there is a wetting trend on both sides of

the line, especially in Xinjiang and Qinghai. The results of Wu's research showed an obvious pattern in the climate risk regression map (based on the comprehensive aridity index) that the northwest region has a high risk of drought and the southeast region has a high risk of waterlogging, whereas the area near the Hu-Huanyong Line is mostly mild climate (Wu et al., 2018). And Huang's research showed that the climate (based on SPEI) in the northwest region had a wetting trend whereas some areas near the Hu-Huanyong Line had drought trend (Q. Huang et al., 2017). Research results in other subregions, such as in Songhua River Basin (Song et al., 2015), Pearl River Basin (Zhao et al., 2014), Hengduan Mountains region (K. Zhang et al., 2014), Yangtze River Basin (T. Gao & Xie, 2016), coastal area of China (X. Wang et al., 2017), Xinjiang (J. Yao, Zhao, Chen, Yu, & Zhang, 2018), also had similar conclusions with this study. Different from common urban flooding risk zoning research (Y. Chen et al., 2015; Yin, Yu, Yin, Liu, & He, 2016), this study explored the risk or possibility of flood or drought in Chinese cities in the background of climate change, using cluster analysis to divide the cities according to the characteristics of the conventional and extreme climate events of cities in the future, and analysed the specific types of urban drought and flood risk.

In addition, there are many types of aridity indices, such as SPEI, Palmer Drought Severity Index, and Standardized Precipitation Index, which have been widely applied in previous studies (Vicente-Serrano, Beguería, & López Moreno, 2010; Lloyd-Hughes & Saunders, 2002; Blauhut, Gudmundsson, & Stahl, 2015). However, these drought indices were unable to be used in this study: First, they must depend on the distribution of precipitation or (and) evapotranspiration during the whole period of the study so that the standard reference time domain cannot be extracted. Therefore, the occurrence probability of the same level of drought and flood events of different individuals in the whole-time domain is the same, and there is a lack of comparability among individuals. Second, all these indices meet a particular distribution (e.g., the SPEI value corresponds to a normal distribution with a mean of zero) so that they can only judge the dynamic dry and wet conditions and cannot reflect the long-term average state of individuals.

4.3 | Main uncertainties of this study

The urban drought and flood disaster are affected by many factors, so it is difficult to predict their risk. On the one hand, human activities can change the frequency of disasters. For example, reservoirs have significant impacts on hydrological characteristics (Ming et al., 2017), and rivers controlled by reservoirs may decrease the trend in flood peak discharges and interannual variability (Lajoie, Assani, Roy, & Mesfoui, 2007). At present, China has the largest number (more than 98,000 in 2016) of reservoirs in the world, and one of the main functions of these reservoirs is to regulate and store river water and prevent floods (S. Li et al., 2018). Many studies have shown that the existence of reservoirs can reduce the risk of downstream flood in China (S. Gao et al., 2019; Q. Zhang, Gu, Singh, Xiao, & Chen, 2015). In addition, the change of underlying surface will also affect the ability of cities to cope with extreme precipitation and drought events. Some studies have shown that the environmental benefits of land use in many cities in China tend to increase (Song, Chang, Yang, & Scheffran, 2016), which indicates that the impact of urbanization on drought and flood events will be more complex in the future. On the other hand, climate change is a global problem coupling with the human system and natural system (Bossel, 1999), with numerous and complex influencing factors. It is difficult to predict future climate accurately, for example, models in Coupled Model Intercomparison Project Phase 5 cannot simulate temperature and precipitation well in China; mean annual temperature was underestimated approximately 1.8°C; and mean annual precipitation was overestimated approximately 263 mm by Coupled Model Intercomparison Project Phase 5 (T. X. Yue et al., 2016). But there is no doubt that too little or too much precipitation is the primary cause of urban drought and flood disasters. In view of the uncertainty and unavailability of other data, we only discussed the risk of urban drought and flood caused by local precipitation. The risk analysis based on linear regression can only reflect the future drought and flood risk according to the current climate trend. In addition, meteorological stations record the total precipitation in 1 day, whereas flood events are mostly caused by heavy rain of short timescale that are generally less than 6 hr (Yin et al., 2016). EP on a daily scale cannot necessarily cause urban flood events because of the difference of urban facilities and disaster emergency response capacity. Many real droughts and floods obviously correspond to extreme events in recorded data. For example, according to the Yearbook of Meteorological Disaster in China, Hebei southern plain suffered from severe drought in the first 4 months of 2006, and the meteorological data show that the total precipitation was less than 10 mm during this period in this region. On July 2, 2009, Hengyang city of Hunan province suffered from severe flood, and the precipitation on that day was 151 mm.

In addition, K-means is sensitive to outliers, and the outliers may affect the result of clustering centres and clustering stability (Ye, Cao, Zhang, & Jia, 2016; Yu, Chu, Wang, Chan, & Chang, 2018). We applied APVAI, APVEPF, APVEPI, APVEDF, and APVEDI to cluster analysis, but they have outliers in varying degrees. For example, the value of APVAI range from 0.37 to 50.22, but there are 2,115 cities with APVAI values less than 3.24. That is, in statistics theory, 149 cities (6.58%) belong to outliers, mainly distributed in areas with serious desertification in northwest China. As shown in Figure 6, the spatial distribution of APVAI and its statistical abnormal values (range from 3.24 to 50.22), and after marking the outliers, the spatial distribution of the indexes is more detailed than that of Figure 3b. In addition, the abnormal values of APVEPF, APVEPI, APVEDF, and APVEDI data are accounting for 0%, 1.10%, 3.84%, and 2.21% of the total cities, respectively. However, the main way to deal with outliers is to eliminate them. Because the abnormal performance of the index conforms to the local climate and environment characteristics, this study cannot deal with these outliers. And in the presence of outliers, the results of repeated clustering are consistent, so cluster analysis can be relatively stable.

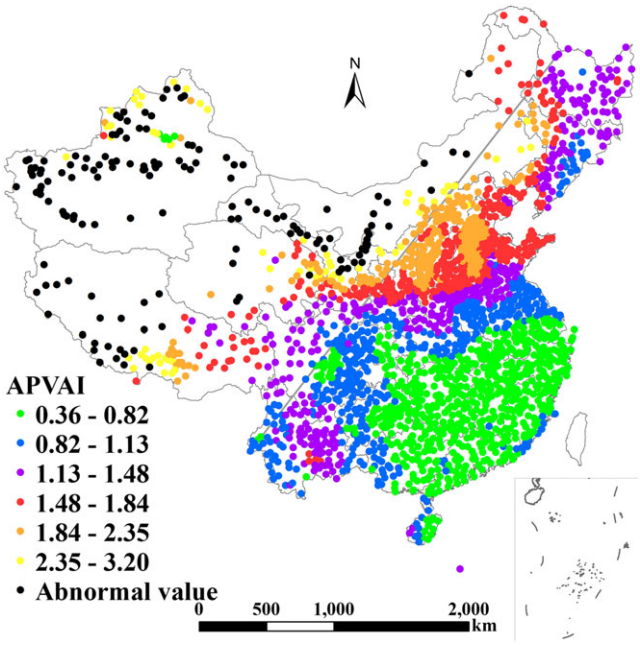

FIGURE 6 The spatial distribution of APVAI and its statistical abnormal value (3.24–50.22). APVAI: average of predicted value of aridity index

5 | CONCLUSION

The characteristics of precipitation, aridity index, extreme precipitation and drought events in 2,264 cities of China were analysed, and the flood and drought risk of the cities were evaluated based on the future short-term forecasts in the context of climate change. We found that precipitation is an important factor affecting AI in most of Chinese cities, and the cities with heavier precipitation tended to have lower AI. Cities with frequent extreme precipitation often have higher intensity of extreme precipitation that are mainly distributed in regions east of the Hu-Huanyong Line, but the extreme drought intensity is often low in cities with high frequency of extreme drought events. The cities with precipitation downward trends are mainly located around the Hu-Huanyong Line. The frequency and intensity trends of extreme precipitation in most cities are the same, as well as the extreme drought. The extreme precipitation events in most cities have become more serious, but the extreme drought events in the cities west of the Hu-Huanyong Line tend to slow down, and the cities east of the Hu-Huanyong Line have a tendency to strengthen. The urban drought and flood risk patterns are distinct, and different types of cities are mainly concentrated in southern China coastal, south of Huaihe, around the Hu Hu-Huanyong Line and Tibet and Xinjiang. Among the six types of cities, the flood risk of Type 1 cities is serious; the drought risk of Type 6 cities is clear; and the characteristics of other cities are more complicated.

ACKNOWLEDGMENTS

This paper was supported by the GDAS' Project of Science and Technology Development (2018GDASCX-0106, 2019GDASYL-0401003, 2019GDASYL-0502004, and 2019GDASYL-0503003), the High-level Leading Talent Introduction Program of GDAS (2016GDASRC-0103), the Guangzhou Science and Technology Plan Project (201707010408), and the Science and Technology Planning Project of Guangdong Province (2017A070702015 and 2017B030314092). We are also grateful to the reviewers and editors.

ORCID

Zaijian Yuan https://orcid.org/0000-0003-2834-8685

REFERENCES

Allen, R. G., Pereira, L. S., Raes, D., Smith, M. (1998). Crop evapotranspiration-guidelines for computing crop water requirements-FAO irrigation and drainage paper 56. Fao, Rome, 300(9): D05109.

Bai, Y. Y., Zhang, Y., He, Z. N., Yang, S. Q., Wu, Z., & Zhao, L. (2013). Influence of urbanization process on the spatial distribution of rainfall over Chongqing metropolitan region. *Meteorological Monthly*, *39*(5), 592–599. (In Chinese)

Bernardini, G., Postacchini, M., Quagliarini, E., Brocchini, M., Cianca, C., & D'Orazio, M. (2017). A preliminary combined simulation tool for the risk assessment of pedestrians' flood-induced evacuation. *Environmental Modelling and Software*, *96*, 14–29. https://doi.org/10.1016/j.envsoft.2017.06.007

Blauhut, V., Gudmundsson, L., & Stahl, K. (2015). Towards pan-European drought risk maps: Quantifying the link between drought indices and reported drought impacts. *Environmental Research Letters*, *10*(1), 014008. https://doi.org/10.1088/1748-9326/10/1/014008

Bossel, H., 1999. Indicators for sustainable development: Theory, method, applications. A Report to the Balaton Group. IISD, Canada. ISBN: 1-895536-13-8. page:80.

Brutsaert, W. (2005). *Hydrology: An introduction*. New York: Cambridge University Press. https://doi.org/10.1017/CBO9780511808470

Budyko, M. I. (1974). *Climate and life* (ed., Vol. 18). *Geophysical Series*. New York: Academic Press.

Chang, L. F., & Huang, S. L. (2015). Assessing urban flooding vulnerability with an emergy approach. *Landscape and Urban Planning*, *143*, 11–24. https://doi.org/10.1016/j.landurbplan.2015.06.004

Chen, Y., Zhou, H., Zhang, H., Du, G., & Zhou, J. (2015). Urban flood risk warning under rapid urbanization. *Environmental Research*, *139*, 3–10. https://doi.org/10.1016/j.envres.2015.02.028

Coumou, D., & Rahmstorf, S. (2012). A decade of weather extremes. *Nature Climate Change*, *2*(7), 491–496. https://doi.org/10.1038/nclimate1452

Dao, N. K., & Hoang, T. T. (2016). Analysis of changes in precipitation and extremes events in Ho Chi Minh City, Vietnam. *Procedia Engineering*, *142*, 229–235.

Du, J., Fang, J., Xu, W., & Shi, P. (2013). Analysis of dry/wet conditions using the standardized precipitation index and its potential usefulness for drought/flood monitoring in Hunan Province, China. *Stochastic Environmental Research and Risk Assessment*, *27*(2), 377–387. https://doi.org/10.1007/s00477-012-0589-6

Du, S., Shi, P., Van Rompaey, A., & Wen, J. (2015). Quantifying the impact of impervious surface location on flood peak discharge in urban areas. *Natural Hazards*, *76*(3), 1457–1471. https://doi.org/10.1007/s11069-014-1463-2

Duan, H. F., Li, F., & Yan, H. (2016). Multi-objective optimal design of detention tanks in the urban stormwater drainage system: LID

implementation and analysis. *Water Resources Management*, *30*(13), 4635–4648. https://doi.org/10.1007/s11269-016-1444-1

Frich, P., Alexander, L. V., Dellamarta, P., Gleason, B., Haylock, M., Tank Klein, A. M. G., & Peterson, T. (2002). Observed coherent changes in climatic extremes during the second half of the twentieth century. *Climate Research*, *19*(3), 193–212. https://doi.org/10.3354/cr019193

Gao, S., Liu, P., Pan, Z., Ming, B., Guo, S., Cheng, L., & Wang, J. (2019). Incorporating reservoir impacts into flood frequency distribution functions. *Journal of Hydrology*, *568*, 234–246. https://doi.org/10.1016/j.jhydrol.2018.10.061

Gao, T., & Xie, L. (2016). Spatiotemporal changes in precipitation extremes over Yangtze River basin, China, considering the rainfall shift in the late 1970s. *Global and Planetary Change*, *147*, 106–124. https://doi.org/10.1016/j.gloplacha.2016.10.016

Gober, P., Sampson, D. A., Quay, R., White, D. D., & Chow, W. T. (2016). Urban adaptation to mega-drought: Anticipatory water modeling, policy, and planning for the urban southwest. *Sustainable Cities and Society*, *27*, 497–504. https://doi.org/10.1016/j.scs.2016.05.001

Golroudbary, V. R., Zeng, Y., Mannaerts, C. M., & Su, Z. B. (2017). Detecting the effect of urban land use on extreme precipitation in the Netherlands. *Weather and Climate Extremes*, *17*, 36–46. https://doi.org/10.1016/j.wace.2017.07.003

Groisman, P. Y., Karl, T. R., Easterling, D. R., Knight, R. W., Jamason, P. F., Hennessy, K. J., … Zhai, P. M. (1999). Changes in the probability of heavy precipitation: Important indicators of climatic change. *Climatic Change*, *42*(1), 243–283. https://doi.org/10.1023/A:1005432803188

Guidolin, M., Chen, A. S., Ghimire, B., Keedwell, E. C., Djordjević, S., & Savić, D. A. (2016). A weighted cellular automata 2D inundation model for rapid flood analysis. *Environmental Modelling and Software*, *84*, 378–394. https://doi.org/10.1016/j.envsoft.2016.07.008

Güneralp, B., Güneralp, İ., & Liu, Y. (2015). Changing global patterns of urban exposure to flood and drought hazards. *Global Environmental Change*, *31*, 217–225. https://doi.org/10.1016/j.gloenvcha.2015.01.002

Guo, Y. R., & Ya, Q. Z. (2014). Urbanization effect on trends of extreme temperature indices of national stations over Mainland China, 1961–2008. *Journal of Climate*, *27*, 2340–2360.

Hallegatte, S., Hourcade, J. C., & Ambrosi, P. (2007). Using climate analogues for assessing climate change economic impacts in urban areas. *Climatic Change*, *82*(1–2), 47–60. https://doi.org/10.1007/s10584-006-9161-z

Huang, H., Chen, X., Zhu, Z., Xie, Y., Liu, L., Wang, X., … Liu, K. (2017). The changing pattern of urban flooding in Guangzhou, China. *Science of the Total Environment*, *622-623*, 394.

Huang, Q., Zhang, Q., Singh, V. P., Shi, P., & Zheng, Y. (2017). Variations of dryness/wetness across China: Changing properties, drought risks, and causes. *Global and Planetary Change*, *155*, 1–12. https://doi.org/10.1016/j.gloplacha.2017.05.010

Jusuf, S. K., Wong, N. H., Hagen, E., Anggoro, R., & Hong, Y. (2007). The influence of land use on the urban heat island in Singapore. *Habitat international*, *31*(2), 232–242.

Kalnay, E., & Cai, M. (2003). Impact of urbanization and land-use change on climate. *Nature*, *423*(6939), 528–531. https://doi.org/10.1038/nature01675

Kendall, M. G. (1975). *Rank correlation methods*. London: Griffin.

Lajoie, F., Assani, A. A., Roy, A. G., & Mesfoui, M. (2007). Impacts of dams on monthly flow characteristics. The influence of watershed size and seasons. *Journal of Hydrology*, *334*(3–4), 423–439. https://doi.org/10.1016/j.jhydrol.2006.10.019

Li, S., Bush, R. T., Santos, I. R., Zhang, Q., Song, K., Mao, R., … Lu, X. X. (2018). Large greenhouse gases emissions from China's lakes and reservoirs. *Water Research*, *147*, 13–24. https://doi.org/10.1016/j.watres.2018.09.053

Li, Y. Z., Luo, B. L., & Zhou, B. (2015). Impact of urbanization on air temperature change in the Changsha-Zhuzhou-Xiangtan region of Hu'nan. *Journal of Arid Meteorology*, *33*(2), 257–262. (In Chinese)

Liang, P., Ding, Y. H., He, J. H., & Tang, X. (2011). Study of relationship between urbanization speed and change of spatial distribution of rainfall over Shanghai. *Journal of Tropical Meteorology*, *27*(4), 475–483.

Liu, S., Huang, S., Huang, Q., Xie, Y., Leng, G., Luan, J., & Li, X. (2017). Identification of the non-stationarity of extreme precipitation events and correlations with large-scale ocean-atmospheric circulation patterns: A case study in the Wei River Basin, China. *Journal of Hydrology*, *548*, 184–195. https://doi.org/10.1016/j.jhydrol.2017.03.012

Lloyd-Hughes, B., & Saunders, M. A. (2002). A drought climatology for Europe. *International Journal of Climatology*, *22*(13), 1571–1592. https://doi.org/10.1002/joc.846

Macqueen, J. (1967). Some methods for classification and analysis of multivariate observations. *Proceedings of the Fifth Berkeley Symposium on Mathematical Statistics and Probability*, *1*(14), 281–297.

Manley, G. (1958). On the frequency of snowfall in metropolitan England. *Quarterly Journal of the Royal Meteorological Society*, *84*(359), 70–72. https://doi.org/10.1002/qj.49708435910

Mann, H. B. (1945). Nonparametric tests against trend. *Econometrica*, *13*(3), 245–259. https://doi.org/10.2307/1907187

Meesuk, V., Vojinovic, Z., Mynett, A. E., & Abdullah, A. F. (2015). Urban flood modelling combining top-view LiDAR data with ground-view SfM observations. *Advances in Water Resources*, *75*, 105–117. https://doi.org/10.1016/j.advwatres.2014.11.008

Meng, M., Ni, J., & Zhang, Z. G. (2004). Aridity index and its application in geo-graphical study. *Acta Phytoecologica Sinica*, (6), 853–861. (In Chinese)

Middelkoop, H., Daamen, K., Gellens, D., Grabs, W., Kwadijk, J. C. J., Lang, H., … Wilke, K. (2001). Impact of climate change on hydrological regimes and water resources management in the Rhine basin. *Climatic Change*, *49*(1), 105–128. https://doi.org/10.1023/A1010784727448

Miller, J. D., & Hutchins, M. (2017). The impacts of urbanization and climate change on urban flooding and urban water quality: A review of the evidence concerning the United Kingdom. *Journal of Hydrology: Regional Studies*, *12*, 345–362.

Ming, B., Liu, P., Guo, S. J., Zhang, X. Q., Feng, M. Y., & Wang, X. X. (2017). Optimizing utility-scale photovoltaic power generation for integration into a hydropower reservoir by incorporating long- and short-term operational decisions. *Applied Energy*, *204*, 432–445. https://doi.org/10.1016/j.apenergy.2017.07.046

Mishra, V., Ganguly, A. R., Nijssen, B., & Lettenmaier, D. P. (2015). Changes in observed climate extremes in global urban areas. *Environmental Research Letters*, *10*(2), 024005. https://doi.org/10.1088/1748-9326/10/2/024005

Ortega-Gómez, T., Pérez-Martín, M. A., & Estrela, T. (2018). Improvement of the drought indicators system in the Júcar River Basin, Spain. *Science of the Total Environment*, *610*, 276–290.

Pachauri, R. K., Allen, M. R., Barros, V. R., Broome, J., Cramer, W., Christ, R., Dubash, N. K., (2014). Climate change 2014: Synthesis report. Contribution of working groups I, II and III to the fifth assessment report of the Intergovernmental Panel on Climate Change. IPCC.

Palumbo, A., & Mozzarella, A. (1980). Rainfall statistical properties in Naples. *Monthly Weather Review*, *108*(11), 1011–1015.

Penman, H. L. (1948). Natural evaporation from open water, bare soil and grass. *Proceedings of the Royal Society A*, *193*, 120–146.

Ponce, V. M., Pandey, R. P., & Ercan, S. (2000). Characterization of drought across climatic spectrum. *Journal of Hydrologic Engineering*, *5*(2), 222–224. https://doi.org/10.1061/(ASCE)1084-0699(2000)5:2(222)

Qi, W., Liu, S., & Zhao, M. (2015). Study on the stability of Hu Line and different spatial patterns of population growth on its both sides. *Acta Geographica Sinica*, *70*(4), 551–566.

Qian, Q. H. (2016). Present state, problems and development trends of urban underground space in China. *Tunnelling and Underground Space Technology*, *25*, 280–289.

Rosenzweig, C., Solecki, W., Hammer, S. A., & Mehrotra, A. (2010). Cities lead the way in climate-change action. *Nature*, *467*(7318), 909–911. https://doi.org/10.1038/467909a

Shao, W. W., Zhang, H. X., Liu, J. H., Yang, G. Y., Chen, X. D., Yang, Z. Y., & Huang, H. (2016). Data integration and its application in the sponge city construction of China. *Procedia Engineering*, *154*, 779–786. https://doi.org/10.1016/j.proeng.2016.07.583

Shepherd, J. M. (2006). Evidence of urban-induced precipitation variability in arid climate regimes. *Journal of Arid Environments*, *67*(4), 607–628. https://doi.org/10.1016/j.jaridenv.2006.03.022

Smith, L. S., Liang, Q., & Quinn, P. F. (2015). Towards a hydrodynamic modelling framework appropriate for applications in urban flood assessment and mitigation using heterogeneous computing. *Urban Water Journal*, *12*(1), 67–78. https://doi.org/10.1080/1573062X.2014.938763

Song, X., Chang, K. T., Yang, L., & Scheffran, J. (2016). Change in environmental benefits of urban land use and its drivers in Chinese cities, 2000–2010. *International Journal of Environmental Research and Public Health*, *13*(6), 535. https://doi.org/10.3390/ijerph13060535

Song, X., Song, S., Sun, W., Mu, X., Wang, S., Li, J., & Li, Y. (2015). Recent changes in extreme precipitation and drought over the Songhua River Basin, China, during 1960-2013. *Atmospheric Research*, *157*, 137–152. https://doi.org/10.1016/j.atmosres.2015.01.022

Tortajada, C., Kastner, M. J., Buurman, J., & Biswas, A. K. (2017). The California drought: Coping responses and resilience building. *Environmental Science & Policy*, *78*, 97–113. https://doi.org/10.1016/j.envsci.2017.09.012

Vicente-Serrano, S. M., Beguería, S., & López Moreno, J. I. (2010). A multiscalar drought index sensitive to global warming: The standardized precipitation evapotranspiration index. *Journal of Climate*, *23*(7), 1696–1718. https://doi.org/10.1175/2009JCLI2909.1

Vineyard, D., Ingwersen, W. W., Hawkins, T. R., Xue, X., Demeke, B., & Shuster, W. (2015). Comparing green and grey infrastructure using life cycle cost and environmental impact: A rain garden case study in Cincinnati, Oh. *Journal of the American Water Resources Association*, *51*(5), 1342–1360. https://doi.org/10.1111/1752-1688.12320

Wang, H., Shao, Z., Gao, T., Zou, T., Liu, J., & Yuan, H. (2017). Extreme precipitation event over the Yellow Sea western coast: Is there a trend? *Quaternary International*, *441*, 1–17. https://doi.org/10.1016/j.quaint.2016.08.014

Wang, X., Hou, X., & Wang, Y. (2017). Spatiotemporal variations and regional differences of extreme precipitation events in the Coastal area of China from 1961 to 2014. *Atomic Resolution*, *197*, 94–104. https://doi.org/10.1016/j.atmosres.2017.06.022

Wu, Z., Xu, H., Li, Y., Wen, L., Li, J., Lu, G., & Li, X. (2018). Climate and drought risk regionalisation in China based on probabilistic aridity and drought index. *Science of the Total Environment*, *612*, 513–521. https://doi.org/10.1016/j.scitotenv.2017.08.078

Yang, L., Scheffran, J., Qin, H., & You, Q. (2015). Climate-related flood risks and urban responses in the Pearl River Delta, China. *Regional Environmental Change*, *15*(2), 379–391. https://doi.org/10.1007/s10113-014-0651-7

Yang, L. E., Chan, F. K. S., & Scheffran, J. (2018). Climate change, water management and stakeholder analysis in the Dongjiang River basin in South China. *International Journal of Water Resources Development*, *34*(2), 166–191.

Yao, J., Zhao, Y., Chen, Y., Yu, X., & Zhang, R. (2018). Multi-scale assessments of droughts: A case study in Xinjiang, China. *Science of the Total Environment*, *630*, 444–452. https://doi.org/10.1016/j.scitotenv.2018.02.200

Yao, L., Wei, W., & Chen, L. (2016). How does imperviousness impact the urban rainfall-runoff process under various storm cases? *Ecological Indicators*, *60*, 893–905. https://doi.org/10.1016/j.ecolind.2015.08.041

Ye, Z., Cao, H., Zhang, Y., & Jia, L. (2016). Outlier factor based partitional clustering analysis with constraints discovery and representative objects generation. *Neurocomputing*, *173*(P3), 1538–1553. https://doi.org/10.1016/j.neucom.2015.09.027

Yin, J., Yu, D., Yin, Z., Liu, M., & He, Q. (2016). Evaluating the impact and risk of pluvial flash flood on intra-urban road network: A case study in the city center of Shanghai, China. *Journal of Hydrology*, *537*, 138–145. https://doi.org/10.1016/j.jhydrol.2016.03.037

Yu, S. S., Chu, S. W., Wang, C. M., Chan, Y. K., & Chang, T. C. (2018). Two improved K-means algorithms. *Applied Soft Computing*, *68*, 747–755. https://doi.org/10.1016/j.asoc.2017.08.032

Yuan, Z., Liang, C., & Li, D. (2018). Urban stormwater management based on an analysis of climate change: A case study of the Hebei and Guangdong provinces. *Landscape and Urban Planning*, *177*, 217–226. https://doi.org/10.1016/j.landurbplan.2018.04.003

Yue, S., Pilon, P., Phinney, B., & Cavadias, G. (2002). The influence of autocorrelation on the ability to detect trend in hydrological series. *Hydrological Processes*, *16*(9), 1807–1829. https://doi.org/10.1002/hyp.1095

Yue, T. X., Zhao, N., Fan, Z. M., Li, J., Chen, C. F., Lu, Y. M., … Wilson, J. (2016). CMIP5 downscaling and its uncertainty in china. *Global and Planetary Change*, *146*, 30–37. https://doi.org/10.1016/j.gloplacha.2016.09.003

Zhai, P., Zhang, X., Wan, H., & Pan, X. (2005). Trends in total precipitation and frequency of daily precipitation extremes over China. *Journal of Climate*, *18*(7), 1096–1108. https://doi.org/10.1175/JCLI-3318.1

Zhang, A. Y., Ren, G. Y., Zhou, J. X., Chu, Z. Y., Ren, Y. Y., & Tang, G. L. (2010). Urbanization effect on surface air temperature trends over China. *Acta Meteorologica Sinica*, *68*(6), 957–966.

Zhang, K., Pan, S., Cao, L., Wang, Y., Zhao, Y., & Zhang, W. (2014). Spatial distribution and temporal trends in precipitation extremes over the Hengduan Mountains region, China, from 1961 to 2012. *Quaternary International*, *349*, 346–356. https://doi.org/10.1016/j.quaint.2014.04.050

Zhang, Q., Gu, X., Singh, V. P., Xiao, M., & Chen, X. (2015). Evaluation of flood frequency under non-stationarity resulting from climate indices and reservoir indices in the East River basin, China. *Journal of Hydrology*, *527*, 565–575. https://doi.org/10.1016/j.jhydrol.2015.05.029

Zhao, Y., Zou, X., Cao, L., & Xu, X. (2014). Changes in precipitation extremes over the Pearl River Basin, southern China, during 1960-2012. *Quaternary International*, *333*, 26–39. https://doi.org/10.1016/j.quaint.2014.03.060

Zhou, G., Wei, X., Wu, Y., Liu, S., Huang, Y., Yan, J., … Liu, X. (2011). Quantifying the hydrological responses to climate change in an intact

forested small watershed in southern china. *Global Change Biology*, *17*(12), 3736–3746. https://doi.org/10.1111/j.1365-2486.2011.02499.x

Zou, Y., Xu, Y. Q., & Qiu, C. H. (2015). The research on sponge city construction in southern hilly area—A case study of Ningxiang county in Hunan province. *Economic Geography*, *35*, 65–78. (In Chinese).

How to cite this article: Liang C, Li D, Yuan Z, et al. Assessing urban flood and drought risks under climate change, China. *Hydrological Processes*. 2019;1–13. https://doi.org/10.1002/hyp.13405